# Effect of Gate Threshold Swings by ALD-$Al_2O_3$/AlGaN Interfacial Traps in GaN Power HEMT with Multiple Fluorinated Gate Dielectric Layers

Yun-Hsiang Wang[1,4], Yung C. Liang[1,*], Ganesh S. Samudra[1], Bo-Jhang Huang[2], Ya-Chu Liao[2], Chih-Fang Huang[2], Wei-Hung Kuo[3] and Guo-Qiang Lo[4]
[1]Dept. of ECE, National University of Singapore, Singapore 119260; [2]Dept. of EE, National Tsing Hua University, Taiwan; [3]Industrial Technology Research Institute, Taiwan; [4]A*STAR Institute of Microelectronics, Singapore. [*]Contact author email: chii@nus.edu.sg

**Introduction:** Normally-off AlGaN/GaN HEMT is desirable in power applications in terms of system controllability. Fluorine ion ($F^-$) treatment [1] and AlGaN barrier recess [2] on the gate region are two of the approaches to deplete the carriers within the normal 2DEG conduction channel in normally-on HEMT. However, for conventional $F^-$ treatment on AlGaN surface [1], annealing was required after treatment for damage recovery which resulted in the escape of $F^-$ and reduced $V_{TH}$. Unannealed multiple $F^-$ treatments on AlGaN surface and ALD-$Al_2O_3$ gate dielectric combining with partial AlGaN recess reported in [3] allowed high total amount of $F^-$ incorporation at the gate which resulted in a high $V_{TH}$ of +5V.

**Purpose and Significance of Work:** This work attempts to analyze the $Al_2O_3$/AlGaN interfacial quality of annealing-free device with 3 rounds of $CHF_3$-based $F^-$ treatments within 4 layers of $Al_2O_3$ gate dielectric in HEMT which is expected to have good channel conductivity and high $V_{TH}$ at the same time. Benchmarking with devices that underwent pre-fluorination annealing right after 1st layer of $Al_2O_3$ deposition, unannealed device has about 10 times lower shallow interface trap density ($D_{it}$) which resulted in significantly smaller drain leakage current. However, doubled Ulta-violet (UV) -assisted $V_{TH}$ hysteresis ($\Delta V_{TH}$) found in bi-directional $I_D$-$V_G$ sweep indicates higher concentration of deep-level traps without gate stack annealing.

**Results and Discussion:** The device fabrication begins with Ti/Al/Ni/Au (25/125/45/55 nm) ohmic contacts formed by RTA at 850°C for 30s. Then, 500nm-deep mesa isolation is formed by $BCl_3$-based ICP-RIE and 150nm $SiO_2$ dielectric deposition by PECVD. After gate opening at the normally-off region, about 10nm of AlGaN (50% in thickness) was recessed by low power $BCl_3$-based ICP-RIE to reduce the 2DEG concentration without damaging the AlGaN/GaN interface that degrades mobility. After 6.5nm of ALD-$Al_2O_3$ deposition at 250℃ and different post-deposition annealing temperatures for gate recess recovery used on Dies B and C, 3 cycles of $CHF_3$ plasma treatment combining with ALD-$Al_2O_3$ were used for gate stack formation to introduce sufficient $F^-$ charges in the gate region for high $V_{TH}$. Longer treatment period was applied on the top layer to minimize $F^-$ penetration into the 2DEG channel that may create mobility degradation. Considering the $CHF_3$ plasma etching on $Al_2O_3$, the total $Al_2O_3$ thickness of 18.1nm is obtained. Detailed device schematics, SEM of the gate cross-section and gate process parameters are shown in Fig. 1 and Table I. The equivalent $F^-$ sheet concentration of each layers was obtained by fitting the measured $V_{TH}$ with Setaurus TCAD simulations.

Fig. 2 (a) shows the bi-directional transfer characteristics (sweep time=20s) of Dies A~C at $V_D$=8V comparing with D-mode MIS-HEMT with $Al_2O_3$ of 18nm without any gate recess. Slight increase of $V_{TH}$ in positive sweep were found with annealing, shows formation of fixed negative charge after annealing. Additionally, different degree of positive shift in $V_{TH}$ was observed during negative sweep, indicating trapping of electrons at the $Al_2O_3$/AlGaN interface or $Al_2O_3$ bulk after applying high gate bias. Halved $\Delta V_{TH}$ was observed after annealing, proving effective reduction in deep-level $Al_2O_3$/AlGaN interfacial trap charge ($Q_{it}$). Shown in Table II are $Q_{it}$ for Die A~C based on Fig. 2(a) along with the $Q_{it}$ after 10s of UV-illumination (UV wavelength=365nm) to measure even deeper $Al_2O_3$/AlGaN traps. $Q_{it}$ were extracted based on [4] where $Q_{it}=\varepsilon_0\varepsilon_{Al2O3}\Delta V_{TH}/(qt_{Al2O3})$, where $\varepsilon_{Al2O3}$=7, $\varepsilon_0$ is the permittivity in vacuum, q is the electronic charge and $t_{Al2O3}$ is the thickness of $Al_2O_3$ which is shown in Table 1. The bi-directional $I_D$-$V_G$ in log-scale and $I_G$-$V_G$ shown Fig. 2(b) has demonstrated increased drain leakage current under similar gate leakage after annealing.

Fig. 3 (a) compares the DC and pulsed $I_D$-$V_D$ characteristic of Dies A-C at gate overdrive voltage ($V_{GT} = V_G - V_{TH}$) of 10V. For Pulsed $I_D$-$V_D$, it was measured with $V_G$ pulse at −30V for 50ms and 50% duty cycle to examine the current collapse effect due to deep-level electron trapping from gate injection. High $I_{DMAX}$ of 350mA/mm from unannealed Die A under steady state has shown good preservation of 2DEG mobility from $CHF_3$ plasma treatment. Worse current collapse effect obtained from the pulsed I-V measurement for Die A compared with Die B and C shown Fig. 3 (b) agrees with the higher amount of deeper level traps shown in Table II.

Fig. 4 shows the $Al_2O_3$/AlGaN interface trap density ($D_{it}$) distribution from the AlGaN $E_V$ edge obtained from AC conductance method using $D_{it}\approx 2.5(G_p/\omega)_{max}/(Aq)$ [5], where $(G_p/\omega)_{max}$ is maximum value of the ratio between the parallel conductance ($G_p$) and the frequency in radians ($\omega$) at each measured frequency, and A is the area of the gate. Annealing would increase the shallow trap level ($E_T$) density near the $E_C$ edge, while the deeper-level $Q_{it}$ obtained before ($E_T$=0.6eV based on 20s $I_D$-$V_G$ sweep rate) and after ($E_T$=2eV, mid-gap of AlGaN) UV illumination with wavelength of 365nm for 10s shown in Table II decreases with raised annealing temperature.

Fig. 5 explains the effect of carrier trapping & de-trapping mechanisms on $\Delta V_{TH}$ through schematic energy diagram. In Fig. 5 (a) when $V_G$=0V, holes accumulated at AlGaN/GaN interface will be trapped at the shallow $Al_2O_3$/AlGaN trap levels and hopping across the gate region into the channel induces drain leakage current. As more shallow level were found for annealed dies shown in Fig. 4, greater drain leakage current for Dies B & C shown in Fig 2(b) could be explained. When $V_G>V_{TH}=V_1$ in positive sweep shown in Fig. 5(b), electrons from 2DEG will be trapped at $Al_2O_3$/AlGaN interface. Those trapped electrons will be slowly de-trapping back into 2DEG during negative sweep and those charges remained at the $Al_2O_3$/AlGaN interface will deplete the 2DEG that causes positive $V_{TH}$ shift under the same gate bias $V_1$ shown in Fig. 5(c). Thus, a higher amount of deep-level traps will result in greater trapped charges and larger $\Delta V_{TH}$ during the negative sweep.

**Reference**

[1] H. Chen, M. Wang, and Kevin J. Chen, *Electrochem. and Sol. Letters*, vol. 14, pp. H229-H231, 2011.
[2] K-S. Im, J-B. Ha, K-W. Kim, et al., *IEEE Electron Device Lett.*, vol. 31, pp. 192-194, 2010.
[3] H. Huang, Y-H. Wang, Y.C. Liang, et al., SSDM, Tsukuba, Japan 2014.
[4] Y. Hori, Z. Yatabe, and T. Hashizume, J. Appl. Phys., vol. 114, pp. 244503, 2013.
[5] R. Herbert, Y. Hwang, and S. Stemmer, J. Appl. Phys., vol. 108, pp. 124101, 2010.

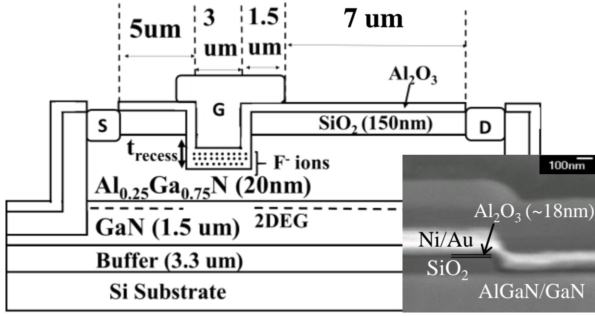


**Fig. 1** Cross-sectional schematics and SEM image of the fabricated device

**Table I.** Steps for gate fabrication of Dies A~C

| Steps | Process | Dies | | |
|---|---|---|---|---|
| | | A | B | C |
| **1** | ALD-$Al_2O_3$ | 6.5 nm | | |
| **2** | Rapid thermal annealing | N/A | 500 ℃ in $N_2$ for 60s | 600 ℃ in $N_2$ for 60s |
| **3** | $F^-$ treatment | $CHF_3$ RIE @ 30W for 140s $F^-$ Conc.~= $-6.51\times10^{12}$ $cm^{-2}$ | | |
| **4** | ALD-$Al_2O_3$ | 7.3 nm | | |
| **5** | $F^-$ treatment | $CHF_3$ RIE @ 30W for 260s $F^-$ Conc.~= $-1.21\times10^{13}$ $cm^{-2}$ | | |
| **6** | ALD-$Al_2O_3$ | 7.6 nm | | |
| **7** | $F^-$ treatment | $CHF_3$ RIE @ 30W for 280s $F^-$ Conc.~= $-1.30\times10^{13}$ $cm^{-2}$ | | |
| **8** | ALD-$Al_2O_3$ | 8 nm | | |
| **Total $Al_2O_3$ thickness considering $F^-$ treatment etching (nm)** | | **18.1 nm** | | |

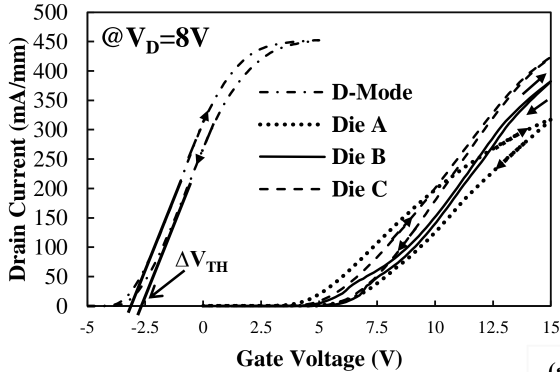


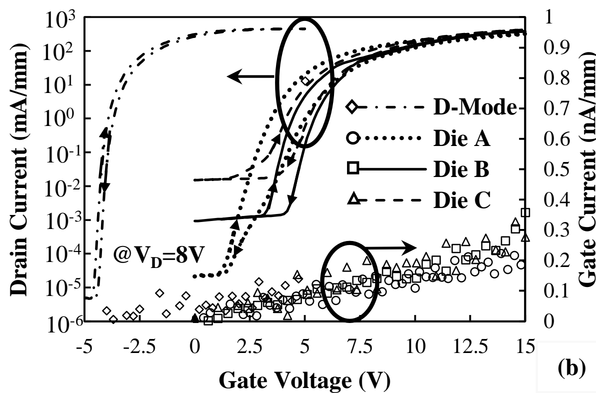


**Fig. 2 (a)** Bi-directional transfer characterisic of Dies A-C with benchmarking D-mode device in linear scale. The sweep was done in clockwise direction in 20s and threshold voltage hysteresis ($\Delta V_{TH}$) is demonstrated. **(b)** Bi-directional transfer characterisic in logarithmic scale and $I_G$-$V_G$ characteristics of Dies A-C and D-mode device. Low gate leakage current has ensured the preservation of insulation quality of the gate dielctric with fluorine treatments.

**Table II.** Extracted threshold voltage hysteresis and $Al_2O_3$/AlGaN interfacial trap of Dies A~C.

| Dies | | D-Mode | A | B | C |
|---|---|---|---|---|---|
| $V_{TH}$ in positive sweep (V) | | -3.0 | 4.8 | 5.4 | 5.5 |
| w/o UV | $\Delta V_{TH}$ (V) | 0.4 | 1.4 | 0.75 | 0.5 |
| | $Q_{it}$ ($10^{12}$ $cm^{-2}$) | 0.86 | 3.01 | 1.61 | 1.08 |
| UV for 30s | $\Delta V_{TH}$ (V) | 0.4 | 2.0 | 1.25 | 1.00 |
| | $Q_{it}$ ($10^{12}$ $cm^{-2}$) | 0.86 | 4.40 | 2.72 | 2.20 |

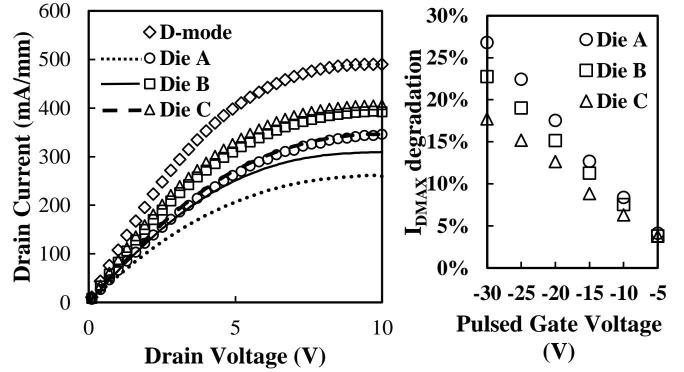


**Fig. 3 (a)** $I_D$-$V_D$ characteristic of Dies A-C with benchmarking normally-on device at gate drive voltage in excess of $V_{TH}$ ($V_{GT}$) of 10V in DC state (datapoints). Pulsed $I_D$-$V_D$ (solid line) measured with $V_G$ pulse at -30V for 50ms and 50% duty cycle is also included. High $I_{DMAX}$ of 400 mA/mm was found for Die C, showing effectiveness of annealing on mobility restoration; **(b)** The amount of $I_{DMAX}$ degradation for pulsed I-V measurement compared with DC I-V results at different pulsed gate voltage. Alleviation in the current collapse effect is found for Die C.

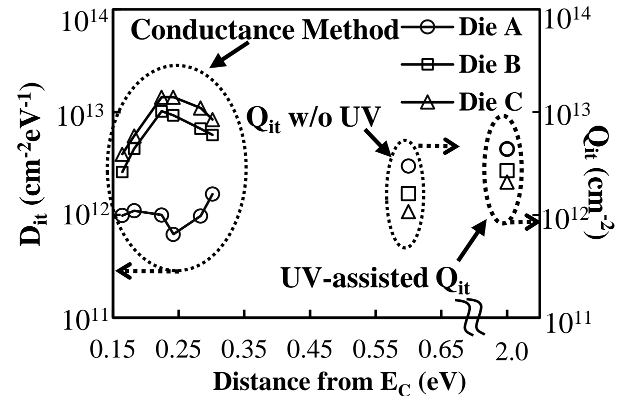


**Fig. 4** $Al_2O_3$/AlGaN interface trap density ($D_{it}$) distribution within the AlGaN energy band obtained from conductance method ($E_T$=0.165 eV to 0.3 eV ) and trapped interface charge $Q_{it}$ from Bi-directional transfer characteristics before ($E_T$=0.6 eV based on 20s $I_D$-$V_G$ sweep rate) and after 10s UV lamp illumination ($E_T$=2 eV) shown in Table II.

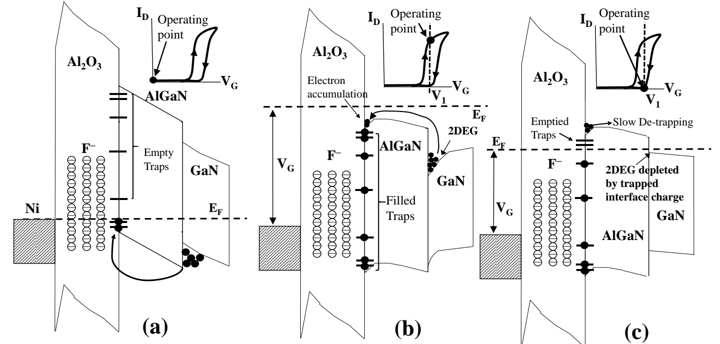


**Fig. 5** Schematic energy band diagram of $Al_2O_3$/AlGaN/GaN interface at **(a)** $V_G$=0V (leakage current induced by hole trapping in shallow $D_{it}$ and hopping across the gate region into the channel) **(b)** $V_G$=$V_1$ in positive sweep (trapping of $Q_{it}$ from 2DEG) and **(c)** $V_G$=$V_1$ in negative sweep (2DEG depletion from $Q_{it}$ resulted in positive $V_{TH}$ shift)

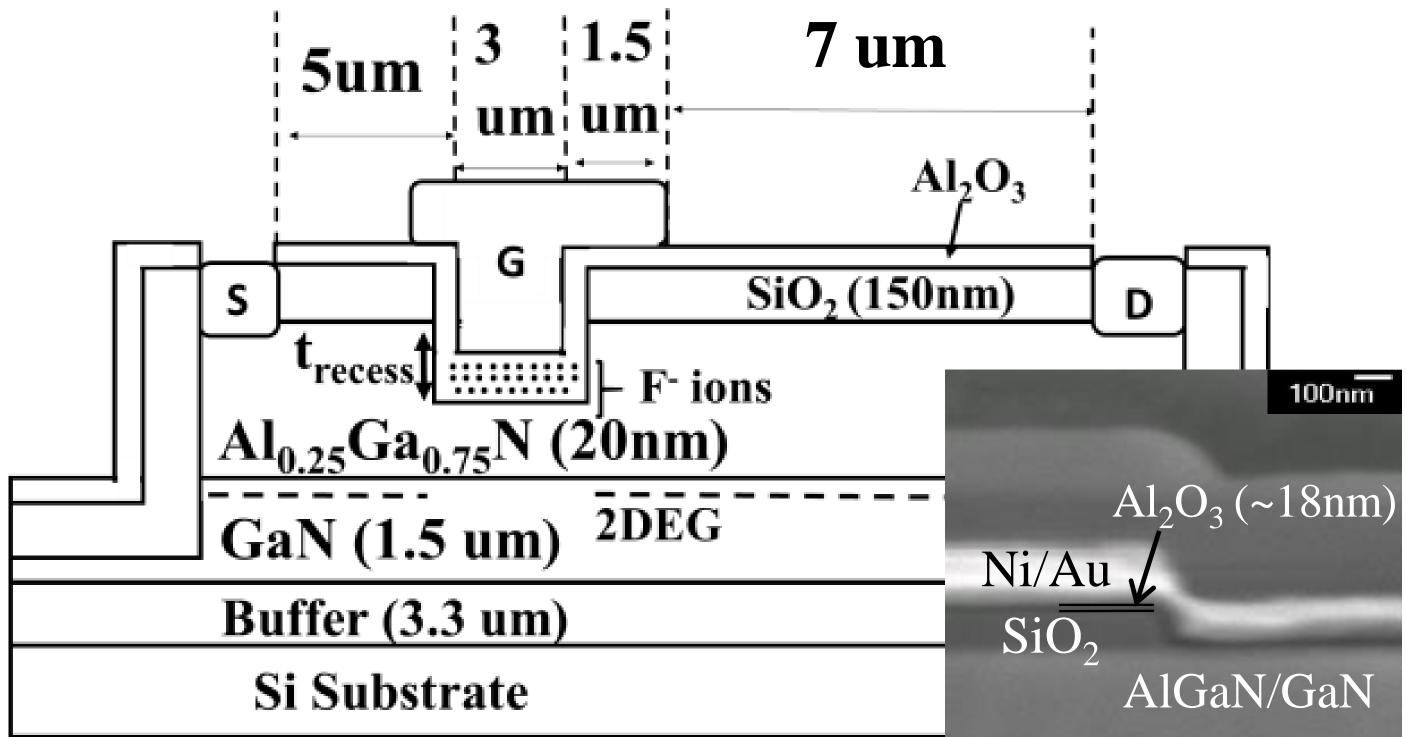


**Fig. 1** Cross-sectional schematics and SEM image of the fabricated device

**Table I.** Steps for gate fabrication of Dies A~C

| Steps | Process | Dies | | |
|---|---|---|---|---|
| | | A | B | C |
| **1** | ALD-$Al_2O_3$ | 6.5 nm | | |
| **2** | Rapid thermal annealing | N/A | 500 ℃ in $N_2$ for 60s | 600 ℃ in $N_2$ for 60s |
| **3** | $F^-$ treatment | $CHF_3$ RIE @ 30W for 140s<br>$F^-$ Conc.~= $-6.51\times10^{12}$ $cm^2$ | | |
| **4** | ALD-$Al_2O_3$ | 7.3 nm | | |
| **5** | $F^-$ treatment | $CHF_3$ RIE @ 30W for 260s<br>$F^-$ Conc.~= $-1.21\times10^{13}$ $cm^2$ | | |
| **6** | ALD-$Al_2O_3$ | 7.6 nm | | |
| **7** | $F^-$ treatment | $CHF_3$ RIE @ 30W for 280s<br>$F^-$ Conc.~= $-1.30\times10^{13}$ $cm^2$ | | |
| **8** | ALD-$Al_2O_3$ | 8 nm | | |
| **Total $Al_2O_3$ thickness considering $F^-$ treatment etching (nm)** | | **18.1 nm** | | |

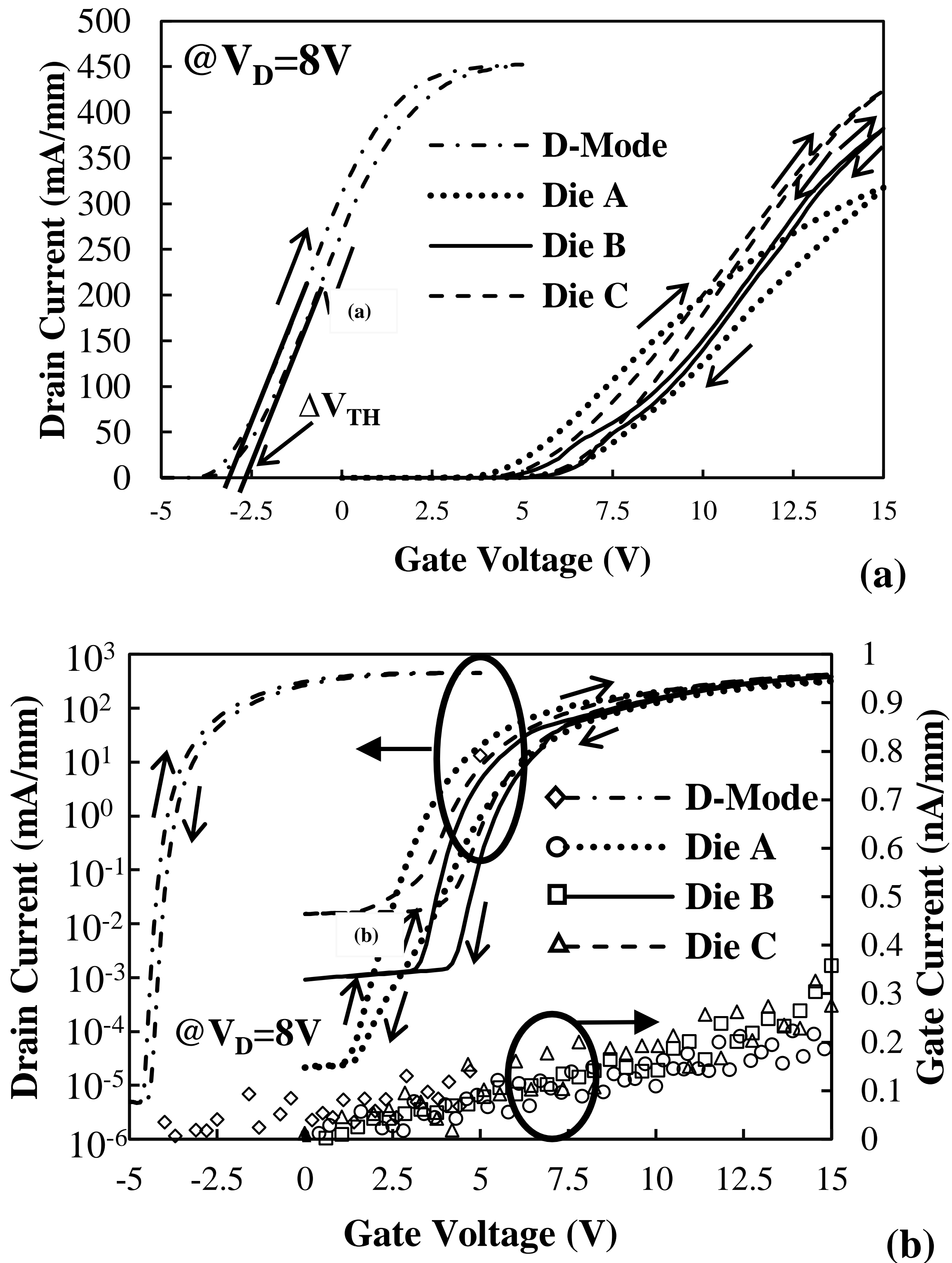


**Fig. 2 (a)** Bi-directional transfer characterisic of Dies A-C with benchmarking D-mode device in linear scale. The sweep was done in clockwise direction and threshold voltage hysteresis ($\Delta V_{TH}$) is demonstrated. **(b)** Bi-directional transfer characterisic in logarithmic scale and $I_G$-$V_G$ characteristics of Dies A-C and D-mode device. Low gate leakage current has ensured the preservation of insulation quality of the gate dielctric with fluorine treatments.

**Table II.** Extracted threshold voltage hysteresis and $Al_2O_3$/AlGaN interfacial trap of Dies A~C.

| **Dies** | | **D-Mode** | **A** | **B** | **C** |
|---|---|---|---|---|---|
| Avg. $V_{TH}$ (V) | | -3.0 | 6.25 | 6.5 | 6.0 |
| w/o UV | $\Delta V_{TH}$ (V) | 0.4 | 1.4 | 0.75 | 0.5 |
| | $Q_{it}$ ($10^{12}$ $cm^{-2}$) | 0.86 | 3.01 | 1.61 | 1.08 |
| UV for 10s | $\Delta V_{TH}$ (V) | 0.4 | 2.0 | 1.25 | 1.00 |
| | $Q_{it}$ ($10^{12}$ $cm^{-2}$) | 0.86 | 4.40 | 2.72 | 2.20 |
| RMS surface morphology of pre-fluorinated $Al_2O_3$ obtained from AFM (nm) | | N/A | 0.65 | 0.50 | 0.30 |

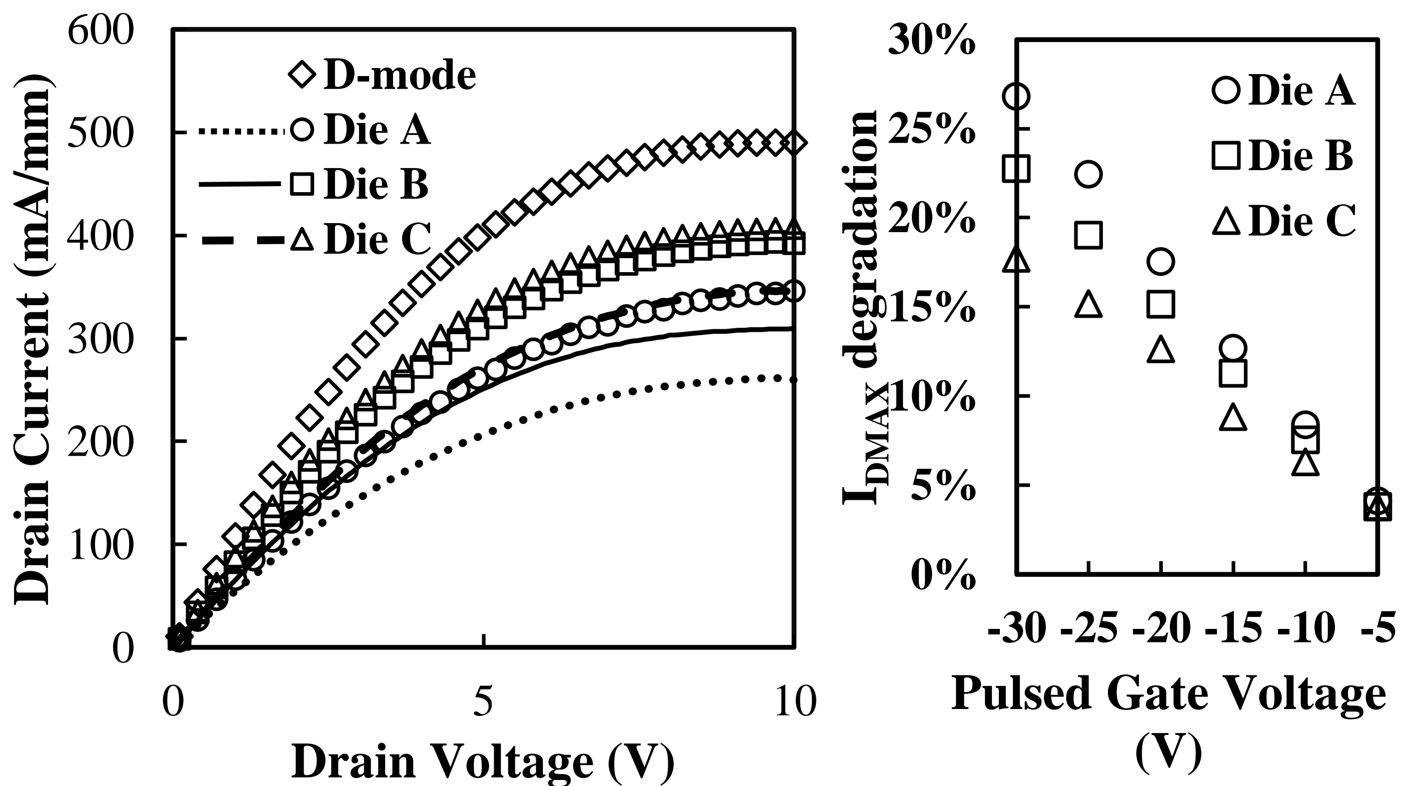


**Fig. 3** (a) $I_D$-$V_D$ characteristic of Dies A-C with benchmarking normally-on device at gate drive voltage in excess of $V_{TH}$ ($V_{GT}$) of 10V in DC state (datapoints). Pulsed $I_D$-$V_D$ (solid line) measured with $V_G$ pulse at -30V for 50ms and 50% duty cycle is also included. High $I_{DMAX}$ of 400 mA/mm was found for Die C, showing effectiveness of annealing on mobility restoration; (b) The amount of $I_{DMAX}$ degradation for pulsed I-V measurement compared with DC I-V results at different pulsed gate voltage. Alleviation in the current collapse effect is found for Die C.

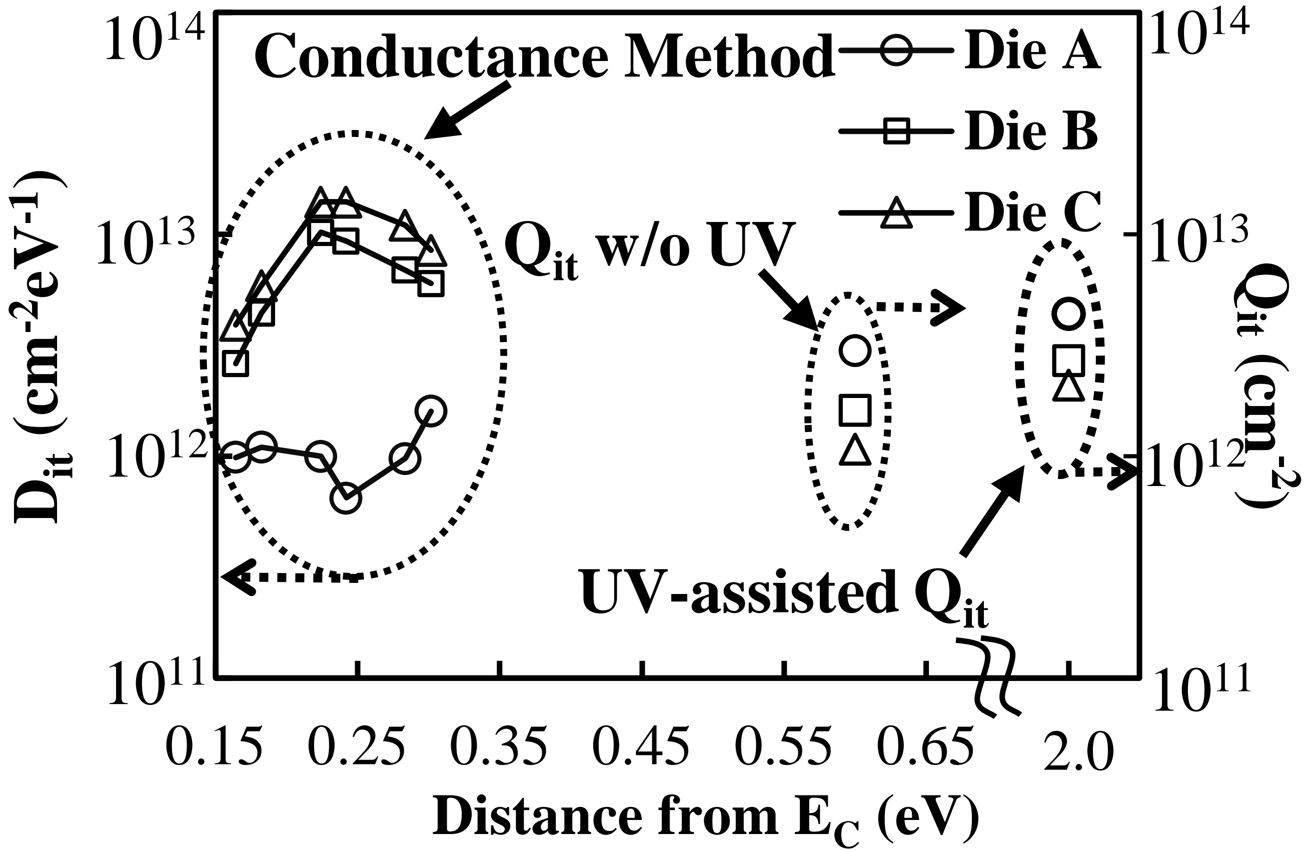


**Fig. 4** $Al_2O_3$/AlGaN interface trap density ($D_{it}$) distribution within the AlGaN energy band obtained from conductance method ($E_T$=0.165 eV to 0.3 eV ) and trapped interface charge $Q_{it}$ from Bi-directional transfer characteristics before ($E_T$=0.6 eV based on 20s $I_D$-$V_G$ sweep rate) and after 10s UV lamp illumination ($E_T$=2 eV) shown in Table II.

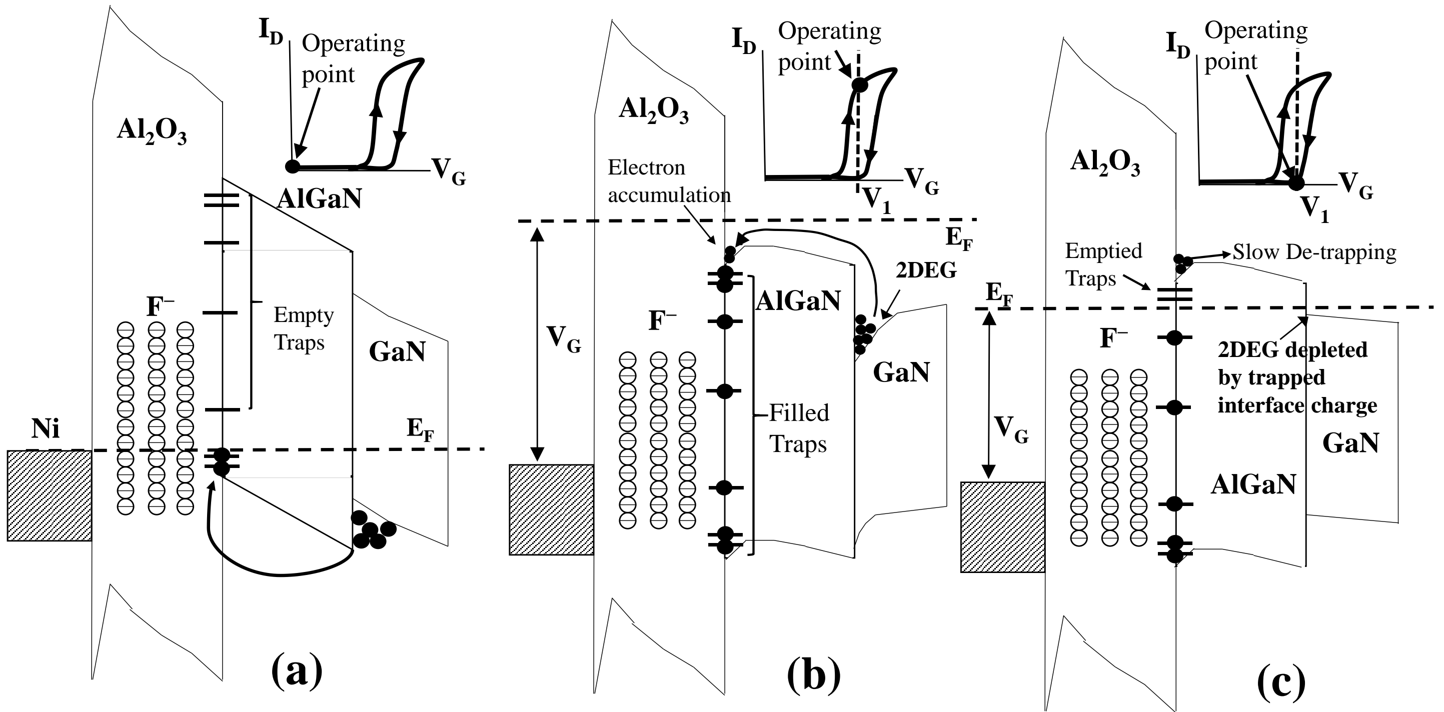


**Fig. 5** Schematic energy band diagram of $Al_2O_3$/AlGaN/GaN interface at **(a)** $V_G$=0V (leakage current induced by hole trapping in shallow $D_{it}$ and hopping across the gate region into the channel) **(b)** $V_G=V_1$ in positive sweep (trapping of $Q_{it}$ from 2DEG) and **(c)** $V_G=V_1$ in negative sweep (2DEG depletion from $Q_{it}$ resulted in positive $V_{TH}$ shift)